Performance Analysis of the Dielectrically Modulated Junction-Less Nanotube Field Effect Transistor for Biomolecule Detection

Shubham Tayal, Budhaditya Majumdar, Member, IEEE, Sandip Bhattacharya, Member, IEEE, and Sayan Kanungo, Senior Member, IEEE

***Abstract*— The design of a high-performance Dielectrically Modulated Field Effect Transistor (DMFET) with smaller device dimension (channel length ≤ 100nm) has recently drawn significant research attention for point-of-care (POC) diagenesis applications. Driven by this paradigm, a Hetero-Gate Metal Dielectrically Modulated Junction-Less Nanotube Field Effect Transistor (DM-JLNFET) architecture is introduced and systematically investigated for label-free electrochemical biosensing application with the help of extensive numerical device simulations. The DM-JLNFET is carefully designed to exploit the advantages of superior gate control over channel electrostatics and electron injection component as well as strong immunity towards the short channel effects that lead to a notably high sensing performance compared to its conventional counterparts. In this context, the underlying physics of the transduction mechanism is analyzed in detail based on the device electrostatics and the carrier transport mechanism. The sensing performance of the proposed biosensor is quantified in terms of the drain current and threshold voltage sensitivities, which represents the relative modulations in these parameters with biomolecule conjugation. Typically, the DM-JLNFET exhibits a drain current and threshold voltage sensitivities as high as 1×10^{12} and 0.70, respectively, for biomolecule dielectric constant above 2. Furthermore, the sensing performance demonstrates strong immunities towards non-uniform cavity occupancy. Finally, extensive comparative performance analysis with Dielectrically Modulated Nanowire Field Effect Transistor (DM-NWFET) is performed. The results exhibit that the proposed DM-JLNFET can offer more than 100% and eight orders of magnitude improvements in the threshold voltage and drain current sensitivities, respectively, for a range of small biomolecule dielectric constants.**

***Index Terms*— Biosensors, Dielectric Modulation, Nanotube, Junction-Less FET, MOSFET, TCAD, Sensitivity.**

I. Introduction

The recent developments in the field-effect transistors (FET) based electrochemical biosensor has demonstrated substantial potential for label-free detection of different biomolecules based on their charge states [**1-3**]. The compatibility with complementary metal-oxide-semiconductor process flow and the scope of on-chip integration of FET biosensors are considered highly encouraging for the lab-on-chip (LOC) based point-of-care (POC) diagnosis applications [**2-4**]. Furthermore, the integration of different emerging nanostructures for such FET-based biosensor design leads to significant improvement in the sensitivity and limit of detection (LOD) [**5-7**]. In this context, the dielectrically modulated FET (DMFET) architectures draw more and more attention from the biosensor research community. The interest in this class of biosensors is due to their ability to detect both charge-neutral and charged biomolecules [**8-10**]. The DMFET biosensors structures are designed with a thicker gate insulator region, wherein a nano-gap cavity is introduced and functionalized with appropriate bio-receptors that have a specific affinity towards target biomolecules (analyte). Consequently, after incubation, the analyte selectively binds itself with the receptors in the cavity region, leading to a modulations in the effective dielectric constant and surface charge density of this region. This results in a change in gate electrostatic coupling with the channel region and thereby the terminal currents of DMFET for detection and quantifications of target biomolecules. Similar to charge-modulated biosensor design, different nanostructures including nanowires [**11-12**], nanosheets [**13-14**], nanotubes [**15-16**], and bio-tubes [**17**] are being actively explored to realize robust and high-performance DMFET designs. Typically, unlike nanowires/nanosheets structures, nanotubes' inner and outer surfaces are available for interactions with target biomolecules, which results in a superior sensing performance in nanotube FET-based biosensors [**15-16**]. However, the successful synthesis and sensor device fabrication using nanomaterials such as Graphene, Silicene, Phosphorene, and transition metal di-chalcogenides nanotubes are technologically challenging and often suffer from the lack of stability in the environment [**18-**

This work has been supported in part by an Outstanding Potential for Excellence in Research and Academics (OPERA) Grant by BITS-Pilani, India and Start-up Research Grant (SRG) by DST-SERB (Grant No. SRG/2020/000547) awarded to Sayan Kanungo.

Shubham Tayal and Sandip Bhattacharya are with the Department of Electronics and Communication Engineering, SR University, Warangal, Telangana- 506371, India.

Budhaditya Majumdar is with the School of Engineering, Macquarie University, NSW-2109 Australia.

Sayan Kanungo, (corresponding author e-mail: ksayan_29@yahoo.co.in) are with the Dept. of Electrical and Electronics Engineering and Materials Center for Sustainable Energy & Environment, Birla Institute of Technology and Science- Pilani, Hyderabad, Telangana - 500078, India.

19]. This motivated the exploration of conventional Silicon (Si) based nanotube-based FET, which exploits its superior gate electrostatics for different applications [20-21]. In Si nanotube-based DMFET architecture, the channel is wrapped around an inner gate terminal, and an outer gate terminal further surrounds the channel region. The nano-gap cavity regions are introduced by carefully etching the thick insulator regions around the gate terminals [22, 15-16]. The target biomolecules can selectively bind with the specific bio-receptors in the cavities, which leads to a measurable change in the device's terminal current and threshold voltage, which is exploited for biomolecule detection [22].

On the other side, it has been observed that the performance of conventional DMFET gets considerably degraded with channel length scaling [23]. Such degradation can be attributed to the higher drain-induced barrier lowering (DIBL) effects in DMFET due to the relatively weaker gate capacitive coupling in the presence of thick nano-gap cavity regions [23-24]. In this context, the junction-less (JL) FET architecture can effectively reduce the DIBL by introducing uniformly doped source, channel, and drain regions. Consequently, the junction-less (JL) DMFET structures are actively explored for biosensing applications [25-26]. In this line, a JL charge/dielectrically modulated bio-tube architecture has been proposed recently. However, the design suffers from a relatively smaller sensitivity towards charged and charge-neutral biomolecules [17]. However, to the best of the authors' knowledge, no attempts have been made to assimilate the advantages of JL-DMFET with nanotube architecture for high-performance sensor device design.

In this work, a novel Dielectrically Modulated Junction-Less Nanotube Field Effect Transistor (DM-JLNFET) architecture has been proposed, and the design is carefully optimized to achieve a significantly superior sensing performance over a range of biomolecule sample specifications. The proposed design exploits both the inherently superior gate control over channel electrostatics in nanotube architecture as well as the favorable carrier injection and strong immunity towards short channel effects in junction-less architecture in favor of transduction. The work comprehensively analyses the essential physics of DM-JLNFET based on source/channel junction electrostatics and thermionic emission at this junction. Subsequently, the influence of applied biasing conditions on the transduction efficiency is studied, and the optimum biasing range of operations is identified. Furthermore, detailed design optimization is performed by tuning the relevant structural parameters. Finally, an extensive comparative performance study is undertaken between Dielectrically Modulated Nanowire Field Effect Transistor (DM-NWFET) and reported

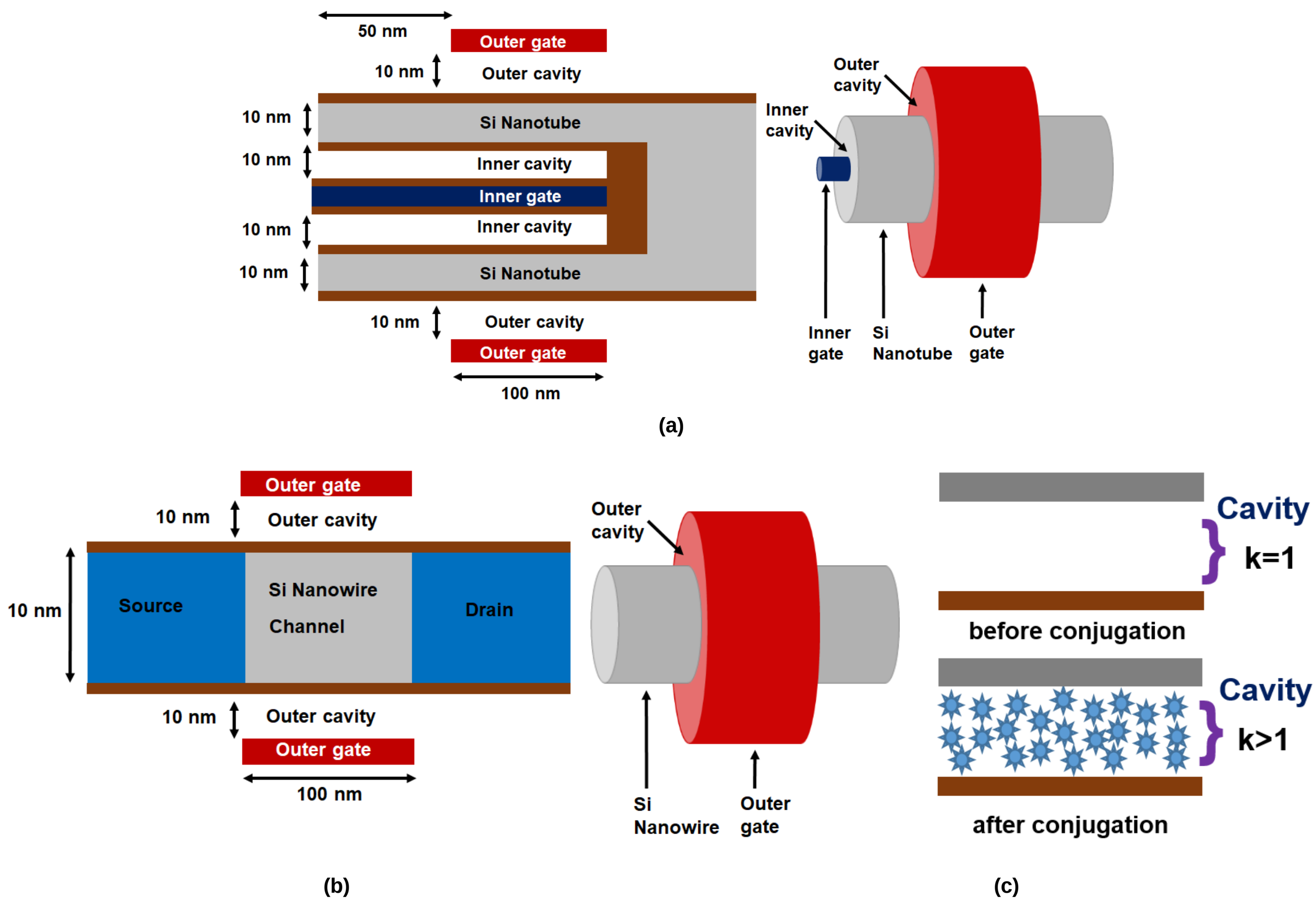

Fig. 1. The Schematic representation and two dimensional cross-sectional views of: (a) Proposed Dielectrically Modulated Junction Less Nanotube FET (DM-JLNFET) biosensors, (b) Conversional Dielectrically Modulated Nanowire FET (DM-NWFET) biosensors including the structural and material specification adopted for simulation in this work, and schematic representation of: (c) biomolecule conjugation in the cavity region and subsequent alteration of effective dielectric constant in the cavity region.

This article has been accepted for publication in a future issue of this journal, but has not been fully edited. Content may change prior to final publication. Citation information: DOI 10.1109/TNB.2022.3172702, IEEE Transactions on NanoBioscience

Dielectrically Modulated Field Effect Transistor (DM-FET), which conclusively demonstrates the superiority of the proposed DM-JLNFET architecture for label-free biosensing applications.

II. Device structure and simulation setup

A. Device Structure and Specifications

The three-dimensional (3D) schematics and the two-dimensional (2D) cross-sectional view of the proposed DM-JLNFET and Dielectrically Modulated Nanowire Field Effect Transistor (DM-NWFET) are illustrated in Fig.1 (a), and (b), respectively. In this work, the gate all around (GAA) architecture is considered to exploit its superior electrostatics integrity in favor of dielectric/charge modulation [**20**, **27**]. The thickness of inner gate and outer gate cavity regions has been considered as 10 nm, according to previous numerical simulation-based reports on dielectrically modulated biosensors [**28-30**]. Furthermore, 1 nm thin insulator (SiO_2) regions are introduced in the inner and outer cavity regions to ensure effective electrical isolation between the active region of the device and the biomolecules [**16, 22, 31**]. However, it is worth mentioning that in the experimental condition, the electrical isolation may be realized by using a thicker high-k insulating material keeping the effective oxide thickness near 1nm. The detailed structural specifications of DM-JLNFET and DM-NWFET are illustrated in Table. I.

Table. I. Structural Specifications of DMFETs

Structural Specifications	**DM-JLNFET**	**DM-NWFET**
Channel Length	100 nm	100 nm
Source/Drain Length	50 nm	50 nm
Channel thickness	10 nm	10 nm
Channel Doping (uniform)	1×10^{19} cm^{-3} (n-type)	1×10^{15} cm^{-3} (p-type)
Source Doping (uniform)	1×10^{19} cm^{-3} (n-type)	1×10^{19} cm^{-3} (n-type)
Drain Doping (uniform)	1×10^{19} cm^{-3} (n-type)	1×10^{19} cm^{-3} (n-type)
Inner-gate cavity thickness	10 nm	-
Outer-gate cavity thickness	10 nm	10 nm
Inner-gate cavity length	150 nm	-
Outer-gate cavity length	100 nm	100 nm
Inner-gate Metal Work-function	4.1 eV (Aluminum)	-
Outer-gate Metal Work-function	5.6 eV (Palladium)	5.6 eV (Palladium)

B. Simulation Framework

The numerical device simulations are performed using commercially available Sentaurus TCAD from Synopsys [**33**].

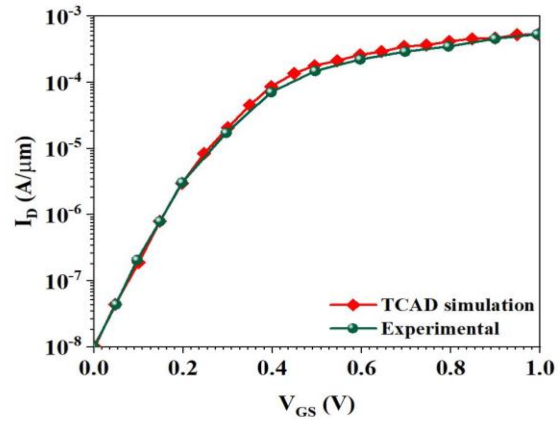

Fig. 2. Calibration plot of experimentally reported [**32**] and TCAD simulated transfer characteristics of Silicon NWFET (having 10 nm gate length, 10 nm nanowire diameter, 1×10^{18} cm^{-3} p-type channel doping, and 1.9 nm effective gate oxide thickness) for V_{DS} = 1.0 V.

The carrier transport mechanism is incorporated using the drift-diffusion model [**33**]. The Fermi-Dirac carrier distribution is considered with the doping-dependent band-gap narrowing and the mobility degradation models to capture the complete effects of high doping concentrations on the electrical characteristics [**33**]. The normal electric field-dependent mobility degradation models are also incorporated to reliably manifest the influence of applied gate bias on the electrical conductivity [**33**]. Furthermore, the Augur and Schottky-Read-Hall (SRH) generation and recombination models are considered in the simulation [**33**]. Finally, the simulation setup of this work is calibrated with experimentally reported Silicon NWFET, which results in a reasonable agreement between TCAD simulated and experimentally reported I-V characteristics, as shown in Fig. 2 [**32**].

Next, in accordance with the previous numerical device simulation based reports on dielectrically modulated biosensors, a suitable insulating material is considered in the cavity regions [**8, 12, 23-28**]. Furthermore, the dielectric constant (k) and surface charge density (ρ) of this insulating material is tuned accordingly, which represent the effects of charge/dielectric modulations over the device electrostatics and carrier transport mechanism [**12-16, 23-28**]. Such a simplified simulation approach is widely used in numerical device simulation-based reports as it offers satisfactory qualitative agreement with experimental results for dielectrically modulated biosensors [**8-9, 34**]. In this work, the absence of biomolecules in the cavity is represented by an air environment (k = 1, ρ = 0). Also, unless otherwise stated, the biomolecule conjugation is represented by the dielectric constant of 2.1 (ρ = 0) throughout the cavity regions. This specification manifests the presence of the streptavidin/biotin binding system in the cavity, which is one of the strongest known non-covalent binding [**8**]. In this context, different biomolecule specifications including low-hydrated proteins (k = 5), glucose oxidase (k = 3.64), 3-aminopropyltriethoxysilan (k = 3.57), cholesterol oxidase (k = 3.28), streptavidin/biotin (k = 2.1), and silica-binding proteins/ avian influenza (k = 1.9) are considered in this work [**35-36**]. On the other hand, surface

This article has been accepted for publication in a future issue of this journal, but has not been fully edited. Content may change prior to final publication. Citation information: DOI 10.1109/TNB.2022.3172702, IEEE Transactions on NanoBioscience

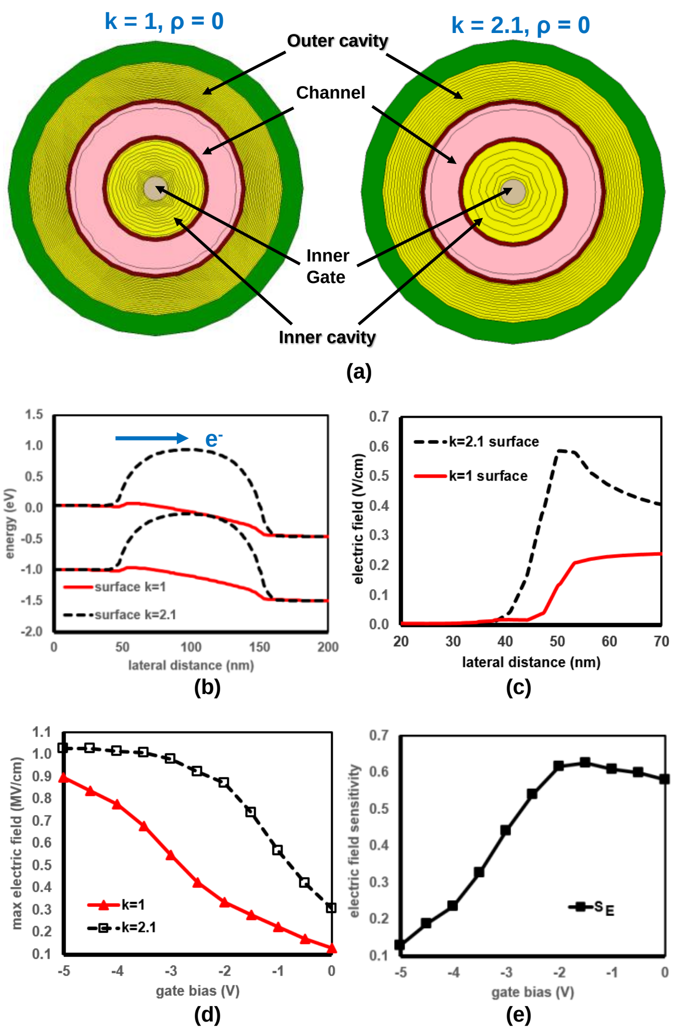

Fig. 3. Plots of: (a) electrostatic potential contour at the middle of the channel from vertical cross-sectional view (b) lateral surface electric field profiles, (c) lateral energy band profiles, at V_{GS} = -1.5 V (d) maximum electric field, and (e) maximum electric field sensitivity (S_E) variation with gate bias, for V_{DS} = 0.5 V DM-JLNFET.

charge density from ρ = 1×10^{11} cm^{-2} to ρ= 1×10^{12} cm^{-2} is considered to represent the effects of DNA hybridization of different concentrations in the cavity [**37-39**].

III. Results and Discussion

A. Device Electrostatics Analysis

Being a JL-FET, the DM-JLNFET architecture incorporates uniform n-type doping concentrations in source, channel, and drain regions [**25-26**]. The n-type channel doping corresponds to a large electron concentration and thereby high electron conductivity in the channel without any applied gate bias (V_{GS}) [**20**]. Consequently, the channel conductivity can be significantly reduced by depleting the channel regions by simultaneously applying a negative potential in the inner and outer gate terminals [**20, 25-26**].

The electrostatic potential contours at the vertical cross-section of the channel region before (k = 1, ρ = 0) and after (k = 2.1, ρ = 0) biomolecule conjugation is illustrated in Fig. 3 (a). In the absence of biomolecules, the denser equipotential lines in the inner and outer cavities indicate that the electrostatic potential drop is at the maximum, which is in agreement with the transduction mechanism of dielectrically modulated biosensors [**28-30**]. Whereas the potential drop in the cavities significantly reduces after biomolecule conjugation, resulting in increasing magnitude (negative) of the channel's surface potentials. The effects of channel surface potential modulation on the carrier transport mechanism have been analyzed from the energy band profiles and surface electric field across the transport direction, and are illustrated in Fig. 3 (b) and (c), respectively. Fig. 3(b) indicates that in the absence of biomolecules, the smaller surface potential at the channel leads to a lower potential barrier for thermionic emission of electrons from the source regions to the channel region, as shown in Fig. 3(c). On the other hand, the presence of biomolecules in the cavity regions increases the channel negative surface potential and raises the potential barrier height at the source/channel junction [**12**]. Consequently, a smaller and larger electric field at the source/channel junction can be observed before and after biomolecule conjugation, respectively, as depicted in Fig. 3(d). The plot suggests that the electron injection flux is strongly correlated with the source/channel junction maximum electric field, as can be observed in other DMFETs [**23**]. Therefore, the maximum electric field is considered before and after biomolecule conjugation for different applied gate biases in Fig. 3(d). The magnitude of electric field modulation with biomolecule conjugation strongly depends on applied gate bias. In this context, the influence of biomolecule conjugation on the thermionic emission mechanism of electrons can be quantified by electric field sensitivity (S_E) at any applied biasing condition, which is defined as:

$$S_E = \frac{E_{bio} - E_{no\_bio}}{E_{no\_bio}} \tag{1}$$

E_{no_bio} and E_{bio} are the maximum surface electric fields at the source/channel junction before and after biomolecule conjugation, respectively. Subsequently, the S_E is considered for a range of V_{GS} and is depicted in Fig. 3(e). Interestingly, the optimum S_E can be observed in the sub-threshold regime of operation for the proposed sensor device, which is usually attributed to the reduced electrostatic screening effects at the channel for FET biosensors [**7, 23**]. This indicates a significant reduction in electron injection flux and terminal current after biomolecule conjugation in the sub-threshold regime.

B. Electrical and Sensing Characteristics

For any FET-based electrochemical sensor, the transduction efficiency depends on the applied gate and drain bias. Therefore, to identify the suitable biasing conditions, the transfer and output characteristics of DM-JLNFET are considered under biomolecule conjugation and are shown in Fig. 4 (a) and (b), respectively. Furthermore, the transduction efficiency of any FET-based sensor is usually quantified by relative variation in the terminal currents and the threshold

This article has been accepted for publication in a future issue of this journal, but has not been fully edited. Content may change prior to final publication. Citation information: DOI 10.1109/TNB.2022.3172702, IEEE Transactions on NanoBioscience

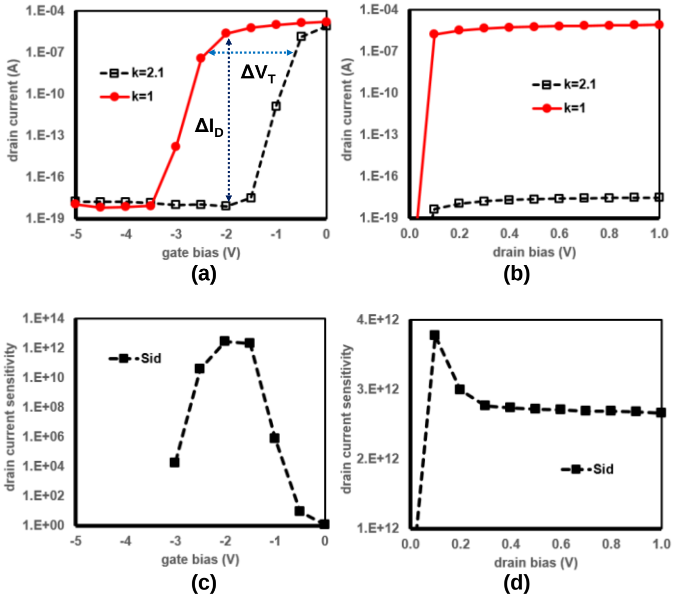

Fig. 4. Plots of: (a) transfer characteristics V_{DS} = 0.5 V (b) output characteristics for V_{GS} = -1.5 V, and maximum drain current sensitivity variation with (c) gate bias for V_{DS} = 0.5 V (d) drain bias for V_{GS} = -1.5 V for DM-JLNFET.

voltages [**5-9**]. Subsequently, the sensing performances of DM-JLNFET is estimated in terms of drain current sensitivity (S_{ID}) and threshold voltage sensitivity (S_{VT}) as follows **[36, 40]**:

$$S_{ID} = \frac{I_{D\_no\_bio} - I_{D\_bio}}{I_{D\_bio}} \tag{2}$$

$$S_{VT} = \frac{V_{T\_no\_bio} - V_{T\_bio}}{V_{T\_no\_bio}} \tag{3}$$

Where, $I_{D\_no\_bio}$ ($V_{T\_no\_bio}$) and I_{D_bio} (V_{T_bio}) are the maximum drain current (threshold voltage) before and after biomolecule conjugation, respectively. The threshold voltages of the sensor devices are considered at the drain current level of 10^{-7} A. It is apparent that the higher the magnitude of these sensitivities, the higher will be the transduction efficiency, which ultimately indicates superiority in dielectrically modulated biosensors design [**29-30**]. It should be further noted that the dB scale definition of current sensitivity [**12**], should lead to similar performance traits as predicted by the conventional sensitivity definition in Eqn. (2) for the proposed biosensor. The S_{ID} as a function of both gate and drain bias is depicted in Fig. 4 (c) and (d), respectively. However, since the S_{VT} is considered at specific biasing conditions, no such plots are incorporated in this case.

Fig. 4 (a) depicts that after biomolecule conjugation, the transfer characteristics experience a large shift towards the origin, which can be quantified from significant threshold voltage reduction. Such a large shift in threshold voltage results in a drain current modulation in the order of the on-state/off-state current ratio for a suitably applied gate bias in the sub-threshold regime of operation for any dielectrically modulated FET biosensors [**28**]. The significant drain current modulation with biomolecule conjugation is retained for different applied drain biases, as shown in Fig. 4 (b). Consequently, the maximum S_{ID} appears at the sub-threshold operation regime, which is a characteristic trait of DMFETs [**17, 20**]. Furthermore, the S_{ID} profile gets flattened around this maximum value, as depicted by Fig. 4 (c). On the other side, Fig. 4(d) represents a quasi-saturation in S_{ID} for small to moderate drain biases, which is also consistent with the previous reports on DMFET [**12**]. This relatively lesser sensitive nature of S_{ID} around its maxima suggests superior stability in the sensing performance of DM-JLNFET.

C. Effects of Structural Parameters Variations

The effects of different structural parameter variations on the transduction efficiency of the DM-JLNFET architecture are comprehensively analyzed and are indicated in Fig. 5. Typically, device doping, gate work-function, and device thickness are identified as the critical design parameters for this study.

The increasing channel doping increases the source/channel junction potential barrier for electron injection in any FET **[12, 23]**. Consequently, after biomolecule conjugation, the electrostatic modulation in the cavity region significantly influences this component leading to a sharp enhancement in S_{ID}, as shown in Fig. 5(a). However, the increased threshold voltage magnitude with channel doping reduces S_{VT}, which is also consistent with the observation of the previous reports on DMFETs [**12**].

Fig. 5(b) indicates marginal and considerable improvements in S_{ID} and S_{VT}, respectively, with increasing outer gate work-function. This can be attributed to the decreasing threshold voltage magnitude with increasing outer gate work-function **[12]**. It should be noted that increasing inner gate work-

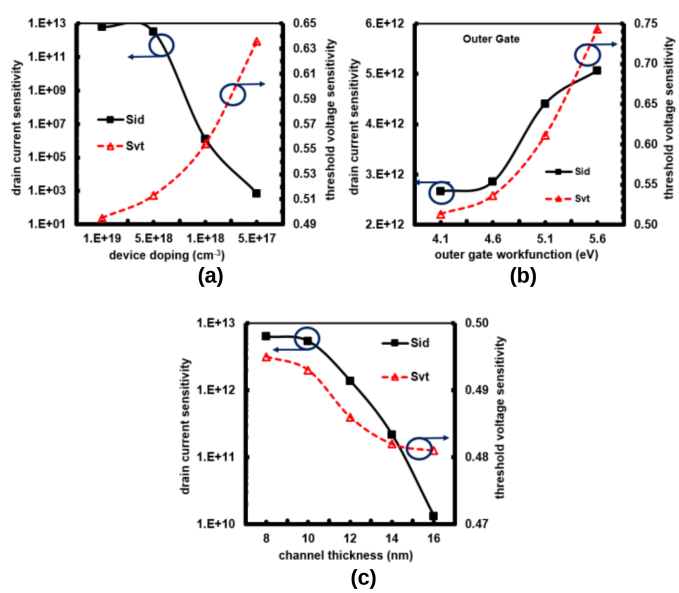

Fig. 5. Plots of maximum drain current sensitivity and threshold voltage sensitivity variation with (a) device doping, (b) outer gate work function, and (c) channel doping for V_{DS} = 0.5 V in DM-JLNFET.

This article has been accepted for publication in a future issue of this journal, but has not been fully edited. Content may change prior to final publication. Citation information: DOI 10.1109/TNB.2022.3172702, IEEE Transactions on NanoBioscience

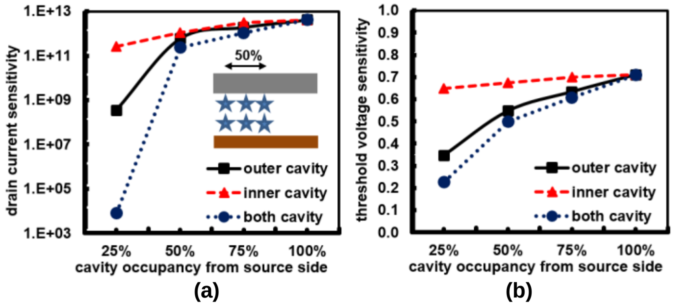

Fig. 6. Plots of: (a) maximum drain current sensitivity and (b) threshold voltage sensitivity variation with partial occupancy of cavity in DM-JLNFET.

function leads to a similar trend with considerably lesser modulations in S_{ID} and S_{VT}, indicating the superior influence of the outer cavity region on the channel electrostatics.

The increasing channel thickness decreases the surface-to-volume ratio, leading to a degradation of gate control over the channel electrostatics in FET **[5, 7]**. Thus, Fig. 5(c) represents a gradual reduction in both S_{ID} and S_{VT} with increasing channel thickness.

In any practical scenario, the spatial distribution of biomolecules inside the cavity regions is usually non-uniform due to surface functionality, binding probability, and steric hindrance effects [**41**]. Consequently, the effects of partially filled cavities on the overall sensing performance of DM-JLNFET are considered, which is illustrated in Fig. 6.

The results indicate that both S_{ID} and S_{VT} are significantly influenced by the spatial distribution of the biomolecules in the cavity region. Typically, the sensing performance remains effectively immune to partial cavity occupancy for the inner cavity alone. The trend suggests the outer cavity electrostatics predominate the overall electrical characteristics of the proposed DM-JLNFET architecture. This also corroborates the previously observed superior influence of outer gate work function dependence on sensing performance. In the context of the spatial distribution of biomolecules within the cavity region, the sensing performance is marginally affected within a 50% to 100% partial outer cavity occupancy from the source side. This trend can be correlated with the fact that the electrons are injected into the channel from the source/channel junction. Subsequently, the channel/drain junction has a marginal influence on the overall sensing performance [**36, 41**]. However, the performance drastically degrades below 50% outer cavity occupancy.

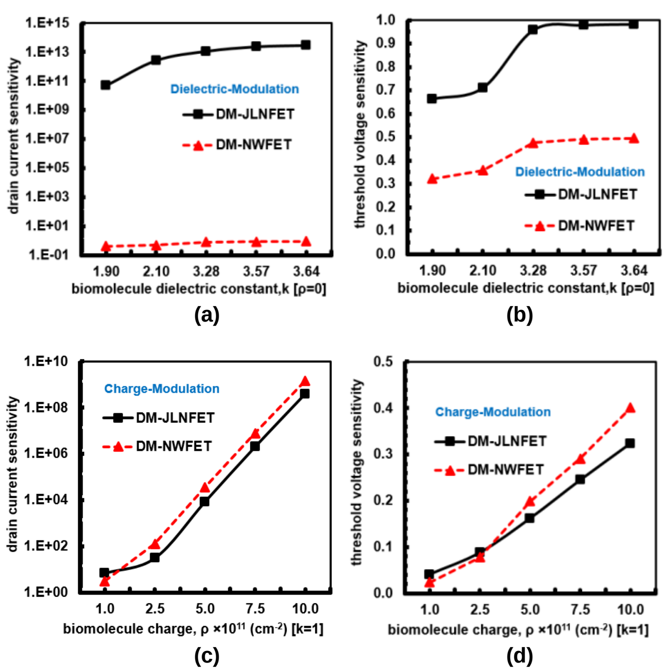

Fig. 7. Comparative plots of: (a) maximum drain current sensitivity and (b) threshold voltage sensitivity variation with biomolecule dielectric constant variation, (c) maximum drain current sensitivity and (d) threshold voltage sensitivity variation with biomolecule charge density variation in DM-JLNFET and DM-NWFET.

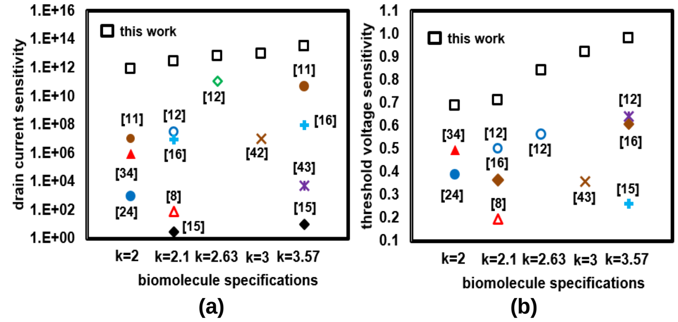

Fig. 8. Plots of: (a) maximum drain current sensitivity and (b) threshold voltage sensitivity in proposed DM-JLNFET and reported DM-FET and DM-NTFET for different biomolecule dielectric constant.

D. Comparative Performance Analysis

Finally, a detailed comparative performance study of the proposed DM-JLNFET is performed with the DM-NWFET of similar structural/material specifications, as shown in Fig.1 (b). Two distinct transduction mechanisms, namely dielectric and charge modulations, are associated with any dielectrically modulated biosensors. Therefore, to gain a clear understanding of the relative merit/demerit of the proposed biosensors, these transduction mechanisms are decoupled by considering only dielectric constant (keeping $\rho = 0$) and charge density (keeping $k = 1$) modulations at a time, as reported in [**36**]. In this context, Fig. 7 indicates the effects of biomolecule specification variations on the S_{ID} and S_{VT} of DM-JLNFET and DM-NWFET.

The results demonstrate that the stronger gate control over the channel electrostatics in DM-JLNFET than DM-NWFET eventually leads to significantly superior sensing performance in the former biosensor for dielectric modulation. Interestingly, the DM-JLNFET slightly underperforms for charge modulation compared to its DM-NWFET counterpart. These findings can be attributed to the larger electrostatic screening at the channel due to higher channel doping in DM-JLNFET, limiting the electrostatic influence of surface charge density modulation in its cavity region. However, it is worth mentioning that a finite change in dielectric constant and charge density are usually associated with any charged biomolecule conjugation [**9**]. Therefore, even for charged biomolecule detection, the slight variation in dielectric constant should ultimately ensure a higher S_{ID} and S_{VT} in DM-JLNFET [**40**].

Finally, to assess the complete merit of the proposed design, the maximum S_{ID} of DM-JLNFET is compared with the existing numerical device simulations based on reports of DM-FETs and Dielectrically Modulated Nanotube Tunnel FET (DM-NTFET) for different biomolecule dielectric constants and is depicted in Fig. 8. The DM-JLNFET is found to surpass the sensing performance of all of the reported DM-FETs and DM-NTFETs considered in this study, which strongly suggests the inherent superiority of the proposed design for label-free biomolecule detection.

IV. Conclusion

In this work, for the first time, a Hetero-Gate Material Dielectrically Modulated Junction-Less Nanotube Field Effect Transistor (DM-JLNFET) architecture is proposed and comprehensively studied for dielectrically modulated label-free biosensing applications. The work demonstrated that the proposed DM-JLNFET design could assimilate the superior electrostatic integrity of the nanotube architecture, as well as highly gate bias sensitive electron injection component and immunity against short-channel effects in junction-less architecture, which leads to a substantial sensing performance improvement in the proposed sensor designed over their reported DMFET and DM-NT-TFET counterparts. Furthermore, the work introduced a suitable gate metal work function difference in the inner and outer cavity regions for optimizing the channel electrostatics and thereby sensing the performance of the proposed DM-JLNFET device. The comparative performance analysis exhibits that the DM-JLNFET is widely surpassing the sensing performance of their previously reported DMFET counterparts. This eventually leads to a distinctly high drain current (threshold voltage) sensitivity of 2×10^{12} (0.71) to 3×10^{13} (0.98) for a small biomolecule dielectric constant over the range of 2.1 to 3.64. In DM-JLNFET, over four orders of drain current sensitivity and more than 30% threshold voltage sensitivity improvements are observed over the conventional DM-NWFET for lower biomolecule dielectric constant. Furthermore, at least an order of magnitude drain current sensitivity and 40% threshold voltage sensitivity improvements are observed over some of the reported DMFETs and DM-NT-TFET architectures. In essence, the work presents detailed theoretical and design insights for the junction-less nanotube FET structures for dielectrically modulated bio-sensing application, which is exploited to systematically optimize the transduction efficiency and ultimately realizing an innovative and highly promising biosensor design.

References

[1] Michael J.Schöning and Arshak Poghossian, "Recent advances in biologically sensitive field-effect transistors (BioFETs)," *The Analyst*, Vol. 127(9), pp. 1137–1151, Aug. 2002. doi:10.1039/b204444g.

[2] Kyungyong Choi, Jee-Yeon Kim, Jae-Hyuk Ahn, Ji-Min Choi, Maesoon Im and Yang-Kyu Choi, "Integration of field effect transistor-based biosensors with a digital microfluidic device for a lab-on-a-chip application," *Lab Chip*, Vol. 12, pp. 1533-1539, Feb. 2012. doi:10.1039/c2lc21203j.

[3] Seokheun Choi, Michael Goryll, Laiyi Mandy Sin, Pak Kin Wong and Junseok Chae, "Microfluidic-based biosensors toward point-of-care detection of nucleic acids and proteins," *Microfluidics and Nanofluidics*, Vol. 10(2), pp. 231–247, June 2010. doi:10.1007/s10404-010-0638-8.

[4] Byungchul Jang, and Arjang Hassibi, "Biosensor Systems in Standard CMOS Processes: Fact or Fiction?,".IEEE Trans. on Industrial Electronics, vol. 56, no. 4, pp. 979- 985, May. 2009. doi: 10.1109/TIE.2008.2011450

[5] Fernando Patolsky and Charles M. Lieber, "Nanowire Nanosensor," materialstoday, vol. 8, issue. 4, pp. 20–28, April. 2005. doi: 10.1016/S1369-7021(05)00791-1

[6] Eric Stern, Robin Wagner, Fred J. Sigworth, Ronald Breaker, Tarek M. Fahmy, and Mark A. Reed, "Importance of the Debye Screening Length on Nanowire Field Effect Transistor Sensors," Nano Letters, vol. 7, no. 11, pp. 3405-3409, October. 2007. doi: 10.1021/nl071792z

[7] Somenath Roy, and Zhiqiang Gao, "Nanostructure-based electrical biosensors," Nano Today, vol. 4, issue.4, pp. 318-334, August. 2009. doi: 10.1016/j.nantod.2009.06.003

[8] Hyungsoon Im, Xing-Jiu Huang, Bonsang Gu and Yang-Kyu Choi, "A dielectric-modulated field-effect transistor for bio-sensing," *Nature Nanotechnology*, Vol. 2(7), pp. 430-434, June 2007. doi:10.1038/nnano.2007.180.

[9] Chang-Hoon Kim, Cheulhoe Jung, Kyung-Bok Lee, Hyun Gyu Park and Yang-Kyu Choi, "Label-free DNA detection with a nano-gap embedded complementary metal oxide semiconductor," *Nanotechnology*, Vol. 22(13), pp. 135502, Feb. 2011. doi:10.1088/0957-4484/22/13/135502.

[10] Maesoon Im, Jae-Hyuk Ahn, Jin-Woo Han, Tae Jung Park, Sang Yup Lee and Yang Kyu Choi, "Development of a Point-of-Care Testing Platform With a Nanogap-Embedded Separated Double-Gate Field Effect Transistor Array and Its Readout System for Detection of Avian Influenza," *IEEE Sensors Journal*, Vol. 11(2), pp. 351–360, Feb. 2011. doi:10.1109/jsen.2010.2062502.

[11] R. Gautam, M. Saxena, R. S. Gupta, and M. Gupta, "Numerical model of gate-all-around MOSFET with vacuum gate dielectric for biomolecule detection," IEEE Electron Device Lett., vol. 33, no. 12, pp. 1756–1758, 494, Dec.2012. doi: 10.1109/LED.2012.2216247

[12] S. Kanungo, S. Chattopadhyay, K. Sinha, P. S. Gupta, and H. Rahaman, "A device simulation based investigation on dielectrically modulated fringing field effect transistor for biosensing applications," IEEE Sensor J., vol. 17, no. 5, pp. 1399–1406, Dec. 2016. doi: 10.1109/JSEN.2016.2633621

[13] A. Shadman, E. Rahman, and Q. D. M. Khosru, "Monolayer MoS_2 and WSe_2 Double Gate Field Effect Transistor as Super Nernst pH sensor and Nanobiosensor," Sensing and Biosensing Research, vol. 11, no. 12, pp. 45-51, Dec. 2016. doi: 10.1016/j.sbsr.2016.08.005

[14] A. Shadman, E. Rahman, and Q. D. M. Khosru, "Quantum ballistic analysis of transition metal dichalcogenides based double gate junctionless field effect transistor and its application in nano-biosensor," Superlattices and Microstructures, vol. 111, no. 11, pp. 414-422, Nov. 2017. doi: 10.1016/j.spmi.2017.06.055

[15] A. Gedam, B. Acharya and G. P. Mishra, "Design and Performance Assessment of Dielectrically Modulated Nanotube TFET Biosensor," IEEE Sensors Journal, vol. 21, no. 15, pp. 16761-16769, Aug. 2021. doi: 10.1109/JSEN.2021.3080922.

[16] S. Shreya, A. H. Khan, N. Kumar, S. I. Amin and S. Anand, "Core-Shell Junctionless Nanotube Tunnel Field Effect Transistor: Design and Sensitivity Analysis for Biosensing Application," IEEE Sensors Journal, vol. 20, no. 2, pp. 672-679, Jan. 2020. doi: 10.1109/JSEN.2019.2944885.

[17] A. Goel, S. Rewari, S. Verma, S. S. Deswal and R. S. Gupta, "Dielectric Modulated Junctionless Biotube FET (DM-JL-BT-FET) Bio-Sensor," IEEE Sensors Journal, vol. 21, no. 15, pp. 16731-16743, Aug. 2021. doi: 10.1109/JSEN.2021.3077540.

[18] Aaron D. Franklin, George S. Tulevski, Shu-Jen Han, Davood Shahrjerdi, Qing Cao, Hong-Yu Chen, H.-S. Philip Wong, and Wilfried Haensch, "Variability in Carbon Nanotube Transistors: Improving Device-to-Device Consistency," ACS Nano, vol. 6, no. 2, pp. 1109-1115, 2012. doi: 10.1021/nn203516z

[19] M. Strojnik, A. Kovic, A. Mrzel, J. Buh, J. Strle, and D. Mihailovic, "MoS2 nanotube field effect transistors," AIP Advances, vol. 4, pp. 097114, 2014. doi: 10.1063/1.4894440

[20] Hossain M. Fahad, Casey E. Smith, Jhonathan P. Rojas, and Muhammad M. Hussain, "Silicon Nanotube Field Effect Transistor with Core–Shell Gate Stacks for Enhanced High-Performance Operation and Area Scaling Benefits," Nano Letters, vol. 11, no. 10, pp. 4393-4399, 2011. doi: 10.1021/nl202563s

[21] H. M. Fahad and M. M. Hussain, "High-Performance Silicon Nanotube Tunneling FET for Ultralow-Power Logic Applications," in IEEE Transactions on Electron Devices, vol. 60, no. 3, pp. 1034-1039, March 2013. doi: 10.1109/TED.2013.2243151.

[22] A. Singh, S. Chaudhary, M. Chanda, and C K Sarkar, "Split gated silicon nanotube FET for bio-sensing applications," IET Circuit, Devices & Systems, vol. 14, no. 8, pp. 1289-1294, Nov. 2020. doi: 10.1049/iet-cds.2020.0208

[23] S. Kanungo, "Introduction to dielectrically modulated biological field effect transistor," 2018 International Symposium on Devices, Circuits and Systems (ISDCS), pp. 1-8, 2018. doi: 10.1109/ISDCS.2018. 8379627.

[24] J. Choi, J. Han, S. Choi and Y. Choi, "Analytical Modeling of a Nanogap-Embedded FET for Application as a Biosensor," in IEEE Transactions on Electron Devices, vol. 57, no. 12, pp. 3477-3484, Dec. 2010. doi: 10.1109/TED.2010.2076152.

[25] Z. Ahangari, "Performance assessment of dual material gate dielectric modulated nanowire junctionless MOSFET for ultrasensitive detection of biomolecules," RSC Adv., vol. 6, pp. 89185-89191, 2016. doi: 10.1039/C6RA17361F

[26] D. Singh and G. C. Patil, "Dielectric-Modulated Bulk-Planar Junctionless Field-Effect Transistor for Biosensing Applications," in IEEE Transactions on Electron Devices, vol. 68, no. 7, pp. 3545-3551, July 2021. doi: 10.1109/TED.2021.3083212.

[27] N. Kumar, U, Mushtaq, S. I. Amin, and S. Anand, "Design and performance analysis of Dual-Gate All around Core-Shell Nanotube TFET," Superlattices and Microstructures, vol. 125, no. 11, pp. 356-364, Nov. 2019. doi: 10.1016/j.spmi.2018.09.012

[28] D. B. Abdi, and M. J. Kumar, "Dielectric modulated overlapping gate-on-drain tunnel-FET as a label-free biosensor," Superlattices and Microstructures, vol. 86, pp. 198-202, Oct. 2015. doi: 10.1016/j.spmi.2015.07.052

[29] R. Goswami and B. Bhowmick, "Comparative Analyses of Circular Gate TFET and Heterojunction TFET for Dielectric-Modulated Label-Free Biosensing," IEEE Sensors Journal, vol. 19, no. 21, pp. 9600-9609, Nov. 2019. doi: 10.1109/JSEN.2019.2928182.

[30] P. Dwivedi and A. Kranti, "Overcoming Biomolecule Location-Dependent Sensitivity Degradation Through Point and Line Tunneling in Dielectric Modulated Biosensors," IEEE Sensors Journal, vol. 18, no. 23, pp. 9604-9611, Dec. 2018. doi: 10.1109/JSEN.2018.2872016.

[31] S. Kanungo, S. Chattopadhyay, P. S. Gupta and H. Rahaman, "Comparative Performance Analysis of the Dielectrically Modulated Full- Gate and Short-Gate Tunnel FET-Based Biosensors," IEEE Transactions on Electron Devices, vol. 62, no. 3, pp. 994-1001, March 2015. doi: 10.1109/TED.2015.2390774.

[32] Yang, F.-L., Lee, D.-H., Chen, H.-Y., et al.: '5 nm-gate nanowire FinFET'. VLSI Technology 2004 Digest Technical Papers 2004 Symp., Honolulu, HI, USA, pp. 196–197, 2004. doi: 10.1109/VLSIT.2004. 1345476

[33] Sentaurus Device User Guide, Version S-2021.06, Synopsys Inc., MountainView, CA, USA, Jun. 2021. [Online].Available: http://www.synopsys.

[34] C. Kim, J. Ahn, K. Lee, C. Jung, H. G. Park and Y. Choi, "A New Sensing Metric to Reduce Data Fluctuations in a Nanogap-Embedded Field-Effect Transistor Biosensor," IEEE Transactions on Electron Devices, vol. 59, no. 10, pp. 2825-2831, Oct. 2012. doi: 10.1109/TED.2012.2209650.

[35] M. Verma, D. Sharma, S. Pandey, K Nigam, and P. N. Kondekar, "Performance comparison of single and dual metal dielectrically modulated TFETs for the application of label free biosensor," Superlattices and Microstructures, vol. 101, pp. 219-227, Jan. 2017. doi: 10.1016/j.spmi.2016.11.045

[36] S. J. Mukhopadhyay, B. Majumdar, K. N. Chappanda, S. C. Mukhopadhyay and S. Kanungo, "Performance Analysis of the Diagonal Tunneling based Dielectrically Modulated Tunnel FET for Bio-sensing Applications," IEEE Sensors Journal, 2021. doi: 10.1109/JSEN.2021. 3103998.

[37] Chang-Hoon Kim, Cheulhee Jung, Kyung-Bok Lee, Hyun Gyu Park and Yang-Kyu Choi, "Label-free DNA detection with a nano-gap embedded complementary metal oxide semiconductor," Nanotechnology, vol. 22, pp. 135502, 2011. doi:10.1088/0957-4484/22/13/135502

[38] P. Venkatesh, K. Nigam, S. Pandey, D. Sharma, P.N. Kondekar, "A dielectrically modulated electrically doped tunnel FET for application of label free biosensor," Superlattices and Microstructures, vol. 109, pp. 470-479, Sept. 2017. doi: 10.1016/j.spmi.2017.05.035

[39] Jae-Hyuk Ahn, Sung-Jin Choi, Jin-Woo Han, Tae Jung Park, Sang Yup Lee, and Yang-Kyu Choi, "Double-Gate Nanowire Field Effect Transistor for a Biosensor," Nano Letters, vol. 10, no. 8, pp. 2934-2938, 2010. doi: 10.1021/nl1010965

[40] S. Kanungo, B. Majumdar, S. Mukhopadhyay, D. Som, S. Chattopadhyay and H. Rahaman, "Investigation on the Effects of Substrate, Back-Gate Bias and Front-Gate Engineering on the Performance of DMTFET-Based Biosensors," IEEE Sensors Journal, vol. 20, no. 18, pp. 10405-10414, 15 Sept.15, 2020. doi: 10.1109/JSEN. 2020.2994295.

[41] Amit Bhattacharyya, Manash Chanda and Debashis De, "Performance Assessment of New Dual-Pocket Vertical Heterostructure Tunnel FET-Based Biosensor Considering Steric Hindrance Issue," IEEE Transactions on Electron Devices,Vol.66(9), pp. 3988–3993, Sept. 2019. doi:10.1109/ted.2019.2928850.

[42] R. Narang, M. Gupta, M. Saxena, and R. S. Gupta, "Analytical model for a dielectric modulated double gate FET (DM-DG-FET) biosensor," in Proc. Int. Conf. Emerg. Electron., Mumbai, India, Dec. 2012, pp. 1–4. doi: 10.1109/ICEmElec.2012.6636256.

[43] J.-H. Ahn, J.-Y. Kim, M. Im, J.-W. Han, and Y.-K. Choi, "A nanogapembedded nanowire field effect transistor for sensing applications: Immunosensor and humidity sensor," in Proc. 14th Int. Conf. Miniaturized Syst. Chem. Life Sci., Groningen, The Netherlands, Oct. 2010, pp. 1301–1303.